STUDY OF MULTIPACTOR DISCHARGE IN THE X-BAND RESONATOR FOR THE ASTERIX PROJECT

M. Mostajeran†[1], L. Faillace[2], A. Gallo[2], D. Alesini[2], Y. Wei[3], Z. Huang[3], B. Spataro[2]

[1]Faculty of Physics, Yazd University, P.O. Box 89195-741, Yazd, Iran
[2]Istituto Nazionale di Fisica Nucleare – Laboratori Nazionali di Frascati, Frascati, Italy
[3]University of Science and Technology of China, Hefei, China

Abstract

Asterix project is a worldwide collaboration involving SLAC, CERN, INFN-LNF, KEK, and Tsinghua University, focused on the study and optimization of advanced X-band (11–12 GHz) accelerating structures. These structures, made of hard copper to ensure better high-gradient performance compared to soft copper, employ various geometries such as open-type cells and use alternative, braze-free joining techniques like TIG welding. The study is driven by the demand for high-gradient accelerating structures capable to sustain gradients above 100 MV/m, which are essential for the next generation of linear accelerators used in research, industrial, and medical applications. An important part of this work is the numerical investigation of multipacting (MP) under different accelerating gradients and geometrical parameters of the quarter– cell model. The simulations performed using CST Studio Suite provided detailed information on how variations in the electromagnetic field amplitude and geometry influence the possible occurrence of MP, allowing for optimization of the structure design and ensuring reliable high-power operation.

INTRODUCTION

Multipactor (MP) occurs when electrons oscillate in the harmonic electromagnetic fields between the walls of a structure and produce new electrons at each impact [1]. If the secondary-electron yield exceeds unit, the electron population grows rapidly and can disrupt the performance of radio-frequency (RF) cavities [2-3]. This phenomenon has been observed in various types of cavities, including high-gradient superconducting cavities and low-frequency coaxial resonators. In X-band structures, which are designed for next-generation accelerators [4], high gradients and small inter-surface distances increase the likelihood of MP.

The purpose of this study is to investigate the conditions of MP in an X-band cavity and to evaluate the effect of the accelerating gradient on the resonant behaviour of electrons. In this work, the cell geometry was initially designed using a four-quadrant symmetrical partition (see Fig. 1). The main geometrical parameters of the cavity are summarized in Table 1. The four-quadrant division allows engineers to simulate only one quadrant and, using symmetry, predict the behaviour of the entire cavity. Subsequent to that, the electromagnetic fields were calculated using the eigenmode solver in CST Microwave Studio (MWS) and transferred to CST Particle Studio (PS) for particle tracking.

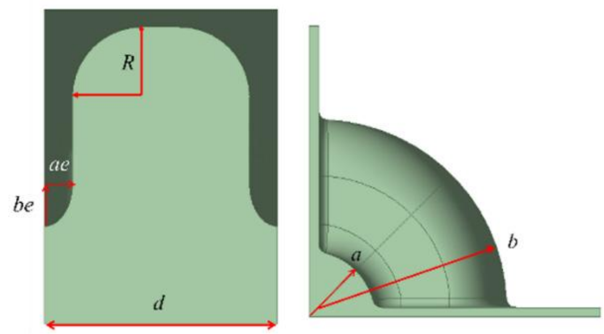

Figure 1: Geometric representation of one quadrant of the cavity (cavity quadrant).

Table 1: Geometrical Parameters of the Cavity

Parameter	Value
Frequency (GHz)	11.994
Gradient(MV/m)	100
Operating mode(rad)	$2\pi/3$
a (mm)	3.5
b(mm)	9.944
ae(mm)	1
be(mm)	1.5
R(mm)	0.5
d(mm)	8.333

SIMULATION METHOD

MP simulation is typically performed in three stages: (1) the structure geometry and RF fields are defined or calculated; (2) the simulation of muli-particle motion in the RF fields and their interaction with the structure walls is performed;(3) the secondary electron emission process is analyzed to assess MP behaviour.

In this work, CST Microwave Studio (MWS) was used to calculate the electromagnetic fields, and CST Particle Studio. (PS), specifically PIC solver was employed for particle tracking and MP analysis. In the CST PS material library, there are number of secondary electron emission models (SEY) for different materials and surface preparations. The annealed copper was selected for this

†mostajeran@yazd.ac.ir

simulation. The Vaughan model was selected for calculating the SEY in this work, Fig.2.

PREPARATION OF THE MODEL FOR PIC SOLVER

The MWS models are defined in vacuum, Fig.3, and do not contain real metallic walls. When transferred to PS, PS cannot recognize these volumes as metallic surfaces and cannot apply secondary-emission properties to them, because such properties are only defined for metallic or plated surfaces. Therefore, a real wall must be introduced into the model.

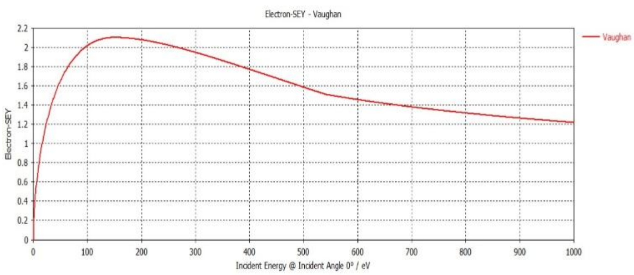

Figure 2: SEY model in CST software.

This is done using the Shell Solid command (see Fig. 4) , which creates a thin shell around a vacuum body. Subsequently, the material with the desired SEY properties is assigned to these walls. The shell thickness must be small and proportional to the model size to avoid geometrical conversion problems. Finally, the RF fields calculated in MWS are imported into the PIC solver, ensuring that that the MP simulation is performed with accurate fields and a correctly defined physical model.

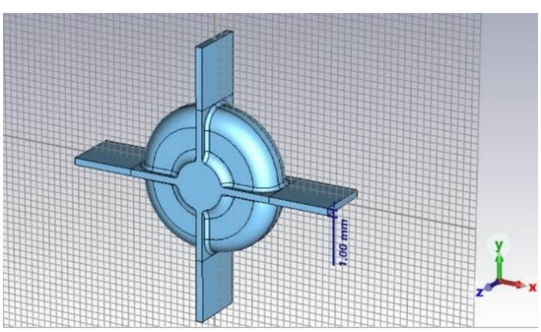

Figure 3: Model of the cavity in MWS.

For the PIC solver, a hexagonal mesh is employed. Unlike tetrahedral meshes in MWS, this type of mesh does not allow selective refinement in different regions; one cannot refine only the mesh in critical areas.

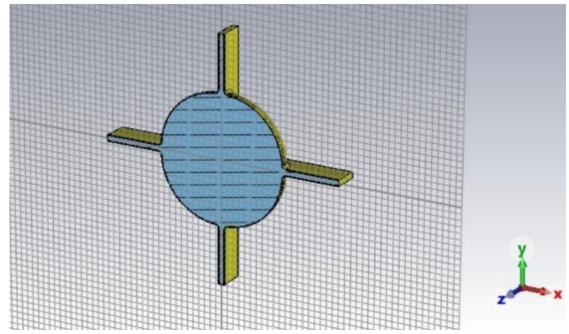

Figure 4: The cavity with surrounding metal walls in the PIC environment.

Consequently, the entire mesh must be sufficiently refined so that particle trajectories are accurately tracked and the field intensity matches that of the eigenmode solutions. If the mesh is too coarse, the field distribution may be erroneous; if it is overly refined, computational resources are unnecessarily consumed. Thus, finding an appropriate mesh density is a key step in simulation accuracy [5].

To evaluate the probability of MP, the phenomenon is examined as a function of the acceleration rate of particles in the cavity. An accelerating voltage is obtained by integrating the longitudinal electric field (E_z)along the cavity axis. Using the eigenmode solver in CST, this integral is calculated, and the effective accelerating voltage (V_{eff}) determined for each cavity. Since the particle velocity is high ($\beta \approx 1$), the accelerating gradient, G, is simply the effective voltage divided by the cavity length ($G = V_{eff} / L$).

The probability of MP is evaluated using the average secondary-emission yield, ⟨SEY⟩, and the collision energy, $W_{collision}$, of particles. Equation (1) defines the average SEY and the collision energy. The collision energies outside the interval 180–610 eV, which correspond to the first and second SEY crossovers of the material, exclude the possibility of MP.

$$< \mathrm{SEY} > \; = \frac{I_{emission}}{I_{collision}}.$$

$$W_{collision}(\mathrm{eV}) = P_{collision}(\mathrm{W}) / I_{collision}(\mathrm{A}). \qquad (1)$$

In CST Particle Studio, standard outputs include particle emission current ($I_{emission}$), collision current ($I_{collision}$), and collision power ($P_{collision}$). These values are used to calculate the average secondary-emission yield (⟨SEY⟩) over the entire simulation time and to calculate the collision power over the last few RF cycles. If ⟨SEY⟩>1 and $W_{collision}$ exceeds 180 eV, it indicates a rapidly increasing number of electrons and the probability of MP occurrence. Typically, in MP simulations, the number of electrons grows exponentially without considering space-charge effects [6].

In the cavity under study, results show that the electron count decreases over time; this reduction indicates that MP does not occur, as shown Figure 5(a) at the accelerating gradient of 100 MV/m. Figure 5(b) shows that ⟨SEY⟩ remains below one across the entire range of accelerating gradients investigated. Figure 5(c) further demonstrates that the mean collision energy with the cavity walls stays far below 180 eV for all gradient values, which is well below the threshold required for MP. Together, these results confirm that multipacting does not occur under the examined conditions.

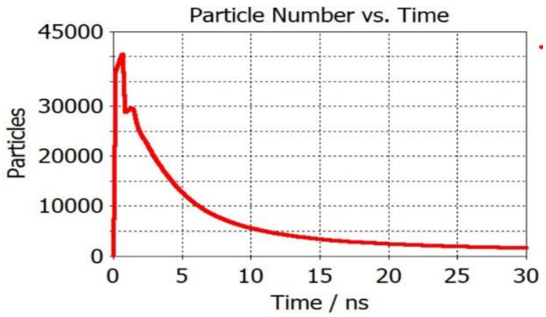

a)

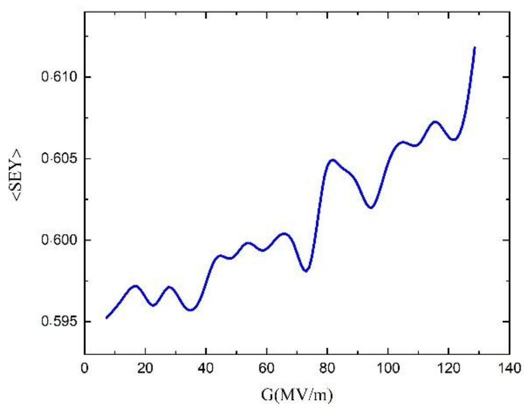

b)

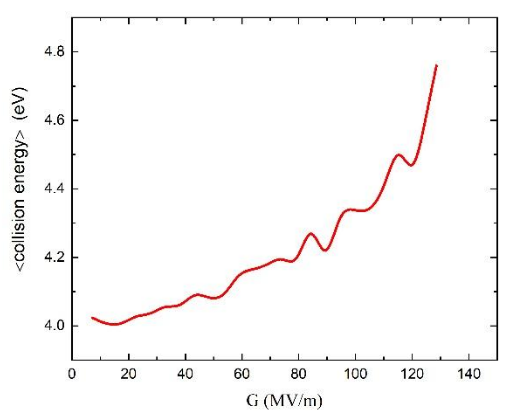

c)

Figure 5: (a) Electron count versus time for G=100 (MV/m); (b) ⟨SEY⟩ as a function of accelerating gradi ent; (c) Average collision energy versus accelerating gra dient.

CONCLUSION

In this study, the MP phenomenon in an X-band accelerator cell of the Asterix project was examined using electromagnetic and particle simulations. Accurate field and secondary-emission analyses revealed no evidence of MP. The average SEY remained below one, and the electron impact energies were below the thresholds needed for ionization. Therefore, the structure studied is free from MP in the examined high-gradient operation and appears stable for high-power applications.

ACKNOWLEDGMENT

Maryam Mostajeran acknowledges the receipt of a fellowship from the ICTP Programme for Training and Research in Italian Laboratories, Trieste, Italy. This work was supported by the Italian National Scientific Committee 5 (CSN5) of INFN under the ASTERIX project. The authors also wish to thank Dr. G. Romanov for the valuable discussions.

REFERENCES

[1] J. R. M. Vaughan, "Multipactor", *IEEE Trans. Electron Devices*, vol. 35, no. 7, pp. 1172–1180, Jul. 1988. https://doi.org/10.1109/16.3387

[2] R. A. Kishek and Y. Y. Lau, "Multipactor discharge on a dielectric", *Phys. Rev. Lett.*, vol. 80, no. 1, pp. 193–196, Jan. 1998. https://doi.org/10.1103/PhysRevLett.80.193

[3] N. F. Kvalev et al., "Scenario for output pulse shortening in microwave generators driven by relativistic electron beams", *IEEE Trans. Plasma Sci.*, vol. 19, no. 3, pp. 246–251, Jun. 1991. https://doi.org/10.1109/27.106820

[4] L. Faillace et al., "High field hybrid photoinjector electron source for advanced light source applications", *Phys. Rev. Accel. Beams*, vol. 25, p. 063401, 2022. https://doi.org/10.1103/PhysRevAccelBeams.25.063401

[5] G. Romanov, "Simulation of multipacting with space charge effect," *Am. J. Phys. Appl.*, vol. 5, no. 6, pp. 99–105, 2017. https://doi.org/10.11648/j.ajpa.20170506.15

[6] F. Kazemi, M. Mostajeran, and G. Romanov, "Analysis of multipacting threshold sensitivity to the random distributions of the secondary electron yield parameters", *Sci. Rep.*, vol. 14, p. 754, 2024. https://doi.org/10.1038/s41598-024-51289-z